Biophysical Journal, Volume 97

Supporting Material

Functional grading of mineral and collagen in the attachment of tendon to bone

Guy M. Genin, Alistair Kent, Victor Birman, Brigitte Wopenka, Jill D. Pasteris, J. Pablo Marquez, and Stavros Thomopoulos

A. Hashin-Shtrikman Bounds

The Hashin-Shtrikman (1963) bounds are the best estimates available for the stiffness of a composite containing uniform dispersions of a reinforcing phase. The equations are reproduced here for convenience. As mentioned in the article, some data from the Monte Carlo simulations fell outside of the Hashin-Shtrikman bounds at the very highest and lowest mineral concentrations considered, since the requirement of uniformity in the distribution of mineral plaques was most heavily violated at these mineral concentrations.

The effective bulk modulus, K_e, of a material containing a volume fraction, f, of collagen (bulk and shear moduli K_c and G_c), and (1-f) of a mineralized collagen (bulk and shear moduli K_{HA} and G_{HA}), is bounded as follows:

$$\frac{1}{\dfrac{f}{\left(\frac{4}{3}G_c + K_{HA}\right)} + \dfrac{1-f}{\left(\frac{4}{3}G_c + K_c\right)}} - \frac{4}{3}G_c \le K_e \le \frac{1}{\dfrac{f}{\left(\frac{4}{3}G_{HA} + K_{HA}\right)} + \dfrac{1-f}{\left(\frac{4}{3}G_{HA} + K_c\right)}} - \frac{4}{3}G_{HA}. \tag{S1}$$

The effective bulk modulus, G_e, is bounded by:

$$\frac{1}{\dfrac{f}{\left(G^*_{\min} + G_{HA}\right)} + \dfrac{1-f}{\left(G^*_{\min} + G_c\right)}} - G^*_{\min} \le G_e \le \frac{1}{\dfrac{f}{\left(G^*_{\max} + G_{HA}\right)} + \dfrac{1-f}{\left(G^*_{\max} + G_c\right)}} - G^*_{\max}, \tag{S2}$$

where

$$G^*_{\min} = G_c\left[\frac{9K_c + 6G_c}{6\left(K_c + 2G_c\right)}\right], \text{ and } G^*_{\max} = G_{HA}\left[\frac{9K_{HA} + 6G_{HA}}{6\left(K_{HA} + 2G_{HA}\right)}\right]. \tag{S3}$$

The bounds on the effective Young's moduli can be calculated using $E_e = 9K_eG_e/(3K_e+2G_e)$.

B. Assessment of the assumption of material linearity for the tendon

Overview: The tendon-to-bone insertion connects tendon, a nonlinear tissue (e.g. Thomopoulos et al., 2003), to bone, a nominally linear tissue. However, the models in this article neglect the nonlinearity of tendon. To assess the impact of this assumption made in the article, we modeled the extreme cases of "parallel" and "series" combinations of tendon and bone in this section. Results indicate that deviations due to nonlinearity are minimal.

Rationale: As in many other material systems with a distributed reinforcing phase (e.g. Torquato, 1991; Marquez et al., 2005), the behavior of the insertion is expected to be near a lower bound at low mineral content (e.g., a Mori-Tanaka (1973) type approximation should be valid), and an upper bound at high mineral content. The Monte Carlo simulations in the current paper show that, within the context of the assumptions tested in this section, mineralized fibers behave similarly.

Methods: Tendon was modeled with Kennedi-type nonlinearity (e.g. Fung, 1993), with an instantaneous uniaxial constitutive response approximated by:

$$\sigma = F(\varepsilon) = a\left(\exp(b\varepsilon) - 1\right), \tag{S4}$$

where a = 1.29 MPa and b = 33.6, and σ and ε are linearized stress and strain measures (Thomopoulos et al., 2003). Bone was treated as linear elastic, with a constitutive response approximated by:

$$\sigma = E_b \varepsilon\,, \tag{S5}$$

where E_b= 20 GPa (e.g. Turner, et al., 1999). Parallel and series (insets, Fig. 7) combinations of bone and tendon were considered over a range of bone volume fractions, V, ranging from 0 (tendon) to 1 (bone), to determine the tangent modulus of the combination, $E_{insertion}$, at a strain of ε_o = 0.025. For the parallel combination, in which the strain carried by the tendinous material equals that carried by the bone-like material the tangent modulus of the insertion at a strain ε_o is:

$$E_{insertion}\Big|_{\varepsilon=\varepsilon_o} = (1-V)ab\exp(b\varepsilon_o) + VE_{bone}\,, \tag{S6}$$

and for the series combination, in which the stress carried by the tendinous material equals that carried by the bone-like material:

$$E_{insertion}\Big|_{\varepsilon=\varepsilon_o} = \left[\frac{1-V}{b(a+\sigma(\varepsilon_o))} + \frac{V}{E_{bone}}\right]^{-1}, \tag{S7}$$

in which $\sigma(\varepsilon_o)$, the stress required to stretch the series combination to ε_o, is found by solving the equation:

$$\cdot\left(\frac{1-V}{b}\right)\ln\left(1+\frac{\sigma(\varepsilon_o)}{a}\right) + \frac{\sigma(\varepsilon_o)}{E_{bone}} = \varepsilon_o\,. \tag{S8}$$

The linear bounds (Reuß and Voigt) are found from Eq. (S6) and (S7) by taking $F(\varepsilon)$ as a linear function, $F(\varepsilon) = E_{tendon}\varepsilon$, where E_{tendon}= 100 MPa is the tangent modulus of tendon at the prescribed level ε_o = 0.025 (Thomopoulos, 2003.)

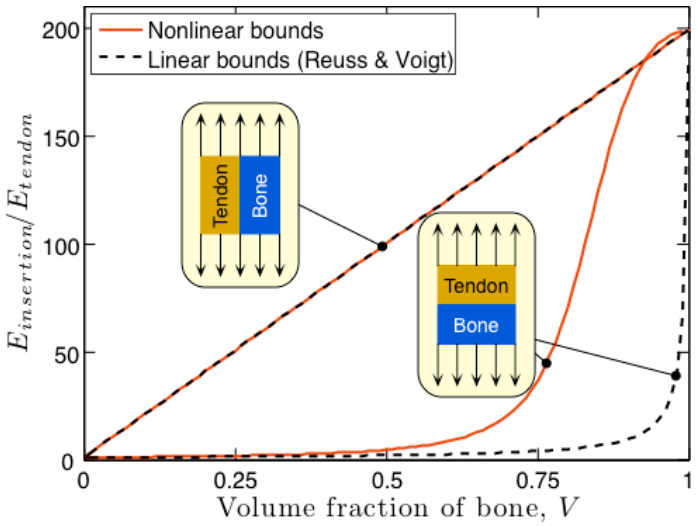

Figure 7. Effect of material nonlinearity on predictions of the tangent modulus of the tendon-to-bone insertion.

Results: The parallel bounds are not affected by material nonlinearity, provided, as was the case in this example, that E_{tendon} was calibrated at the strain level expected in the model insertion (Fig. 7). The series bound was changed little by material nonlinearity at low levels of V, but rose towards the peak at a much lower bone volume fraction when nonlinearity was considered. At some higher mineral volume fractions, the series stiffness prediction exceeded the parallel prediction.

Discussion: This rise in the series bound is expected: as the volume fraction of bone increases, the relative strain in the tendinous material increases, with the result that the effect of material nonlinearity increases. Due to this phenomenon, the "percolation threshold" for partially mineralized collagen fibers would occur at a slightly lower mineral volume fraction had nonlinearity been considered. The predictions made using a linear material model should be accurate at low mineral content, where the solution follows the lower bound, and high mineral content, where the solution follows the upper bound.

C. A slender beam-column is much stiffer in stretching than in flexure

Overview: A somewhat surprising result in the article was that the stiffness of an "imaginary," unmineralized tendon-to-bone insertion drops abruptly when the angular deviation of the fiber orientation distribution exceeds a level of approximately 3° (*cf.* Fig. 5b). In this section, we present a simple model problem we studied to gain insight into this phenomenon. Briefly, we show that when the primary mode of deformation of a slender object such as a drinking straw or a collagen fiber shifts from extension to flexure, the resistance to deformation drops precipitously.

Rationale: Throughout the centerline of the tendon-to-bone insertion, collagen fibers are oriented so that the orientation angle θ relative to the direction of muscle force, averaged over all fibers, 0° (Thomopoulos et al., 2006). However, the distribution of fiber orientations is such that the average fiber will likely point away from the direction of muscle force. The distribution of these angles, quantified by the angular deviation, is higher in the tendon-to-bone insertion and bone than in tendon. We studied the stiffness of a fiber as a function of its orientation angle relative to the direction of muscle force.

Methods: We considered a collagen fiber of length L and radius R, inclined relative to the direction of muscle force at an angle θ, and supported as in Fig. 8. The fiber was linear with axial elastic modulus E_o. We determined the effective modulus of a representative unit cell containing this fiber by considering deformations produced by the downward pulling force shown in Fig. 8.

One component of the applied force, F, deforms the fiber in extension ($F_1 = F\cos\theta$), while the other deforms the fiber in flexure ($F_2 = F\sin\theta$) (Fig. 8).

The effective modulus of elasticity of the fiber was calculated by

$$E_e = \frac{F h_{cell}}{A_{cell}\delta}, \tag{S9}$$

where A_{cell} is the cross-sectional area of the cell shown in Fig. 8 (area of the cylindrical cell perpendicular to the tendon-to-bone insertion centerline $\theta = 0$), $h_{cell} = L\cos\theta$ is the cell height along the centerline, and δ is the elongation of the cell along this centerline produced by the applied force. A_{cell} was evaluated by observing that the volume fraction f_c of the cell is given by $f_c = (A_{fiber}L)/(A_{cell}h_{cell})$, or, rearranging and substituting, $A_{cell} = A_{fiber}L/(f_c h_{cell}) = \pi R^2/(f_c\cos\theta)$. The elongation of the fiber in extension and flexure (in the directions of the forces F_1 and F_2, respectively) are:

$$\delta_1 = \frac{FL\cos\theta}{A_{fiber}E_o} \qquad \text{and} \qquad \delta_2 = \frac{FL^3\sin\theta}{3E_o I}, \tag{S10}$$

respectively, where the second moment of the area about the centerline of the circular fiber is $I = \pi R^4/4$.

The elongation of the cell is now available after straightforward transformations as

$$. \delta = \sqrt{\delta_1^2 + \delta_2^2} = \frac{FL}{\pi R^2 E_o} \sqrt{\cos^2\theta + \frac{16}{9}\left(\frac{L}{R}\right)^4 \sin^2\theta} \,. \tag{S11}$$

Accordingly, Eq. (S9) yields

$$\frac{E_e}{f_c E_o} = \cos^2\theta \left[\cos^2\theta + \frac{16}{9}\left(\frac{L}{R}\right)^4 \sin^2\theta\right]^{-1/2} . \tag{S12}$$

Results: Equation. (S12) was evaluated for a range of angles θ and a fiber aspect ratio L/R = 20 (Fig. 8). As follows from this figure, the local stiffness of the insertion site considered without accounting for the presence of mineral decreased by more than 80% in a 0.5° shift from the direction of muscle force, and another 80% for a 2.5° shift. This decrease is even more pronounced for larger fiber aspect ratios. The sharpest drop in the stiffness is observed at very small values of the orientation angle; i.e., in the cross sections close to the tendon.

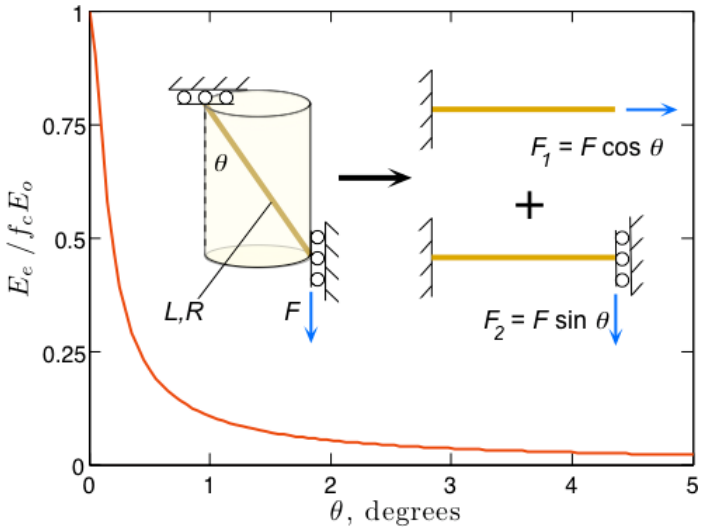

Figure 8. The stiffness of the unit cell pictured drops dramatically as the primary mode of deformation shifts from extension to flexure of the collagen fiber.

Discussion: The stiffness of an un-mineralized tendon-to-bone insertion can be expected to drop precipitously as the average fiber points at an angle further from the direction of muscle force. The mechanism for this drop is a shift in deformation mode from extension (the $\cos^2\theta$ term in the denominator of Eq. (S12)) to flexure (the 16/9 $(L/R)^4 \sin^2\theta$ term in the denominator of Eq. (S12)). The magnitude of the drop is lower in the imaginary unmineralized tendon-to-bone inertion (Fig. 5) than in this example because the unit cells surrounding physiological collagen fibers possess some resistance to deformation in the direction transverse to the fiber axis.